

# Elastic Constant—Porosity Relations for Polycrystalline Thoria

S. Spinner, F. P. Knudsen, and L. Stone

(October 23, 1962)

[The relations between the elastic constants and porosity for about 300 thoria specimens have been determined. Both Young's and the shear modulus for each specimen were obtained by a dynamic resonance method. From these two moduli, Poisson's ratio was computed. The decrease in the elastic constants with increasing porosity was greater than would be expected from the theory. This greater decrease for the experimental values is attributed to the fact that the specimens do not conform to the idealized assumptions of the theory.]

## 1. Introduction

Polycrystalline metals, which are formed by cooling from the molten state, ordinarily result in a material of essentially zero porosity. Consequently, metallurgists who are interested in the relation between microstructure and the macroscopic properties of such materials are generally concerned with the effect of the grains (size, shape, possible orientation) on these (macroscopic) properties. On the other hand, in materials which are formed by sintering—this includes some metals as well as ceramic materials—zero porosity is seldom achieved, so that ceramists studying the relation between microstructure and macroscopic properties of sintered materials must be concerned with the effect of porosity as well as granular structure on macroscopic properties.

The effect of porosity on the elastic properties has been the subject of considerable experimental [1,2,3]<sup>1</sup> and theoretical [4,5,6,7,8] investigation. The primary purpose of the present study is to present data on this relationship (between porosity and elastic constants) obtained from polycrystalline ThO<sub>2</sub> specimens. The reasons for the choice of ThO<sub>2</sub> specimens are twofold. In the first place, very little data of this type are available for ThO<sub>2</sub>. In the second place, since ThO<sub>2</sub> is a cubic crystal, its thermal expansion is isotropic. Consequently, thermally induced intergranular stresses, such as may exist in Al<sub>2</sub>O<sub>3</sub>, for instance, are not present. It would appear, then, that the porosity—elastic constant relationship developed with ThO<sub>2</sub> would come closer to the "ideal" situation. It will be seen later, however, that other complicating factors affected the results to such a degree that this supposed advantage was effectively rendered of minor importance.

## 2. Experimental Procedure

### 2.1. Specimens

All the specimens used in this study were hydrostatically cold pressed and sintered at 1,750 °C for 17 hr. All the specimens were sintered in the same furnace at the same time. The specimens were placed in the center of the (large) furnace in such a manner as to minimize any possible temperature gradients from specimen to specimen. As a further precaution to insure uniform heat treatment, the various groups and subgroups of specimens (to be described) were interspersed in the furnace so that no group would tend to receive a different heat treatment from any other group. A range of porosities was obtained in each of three different groups of specimens in the following manner. In the first group, all the initial particle sizes were from 0 to 2  $\mu$ . The lowest porosity was obtained by using no filler, and increasingly higher porosities were obtained by using increasing amounts of filler in the cold pressing process. The filler burned out on firing. This group is designated as Group I. The second group, designated as Group II, was of 2 to 4  $\mu$  particle size, and the range of porosities was obtained in the same manner. The filler used in all cases consisted of 250–325 mesh unsulfonated styrene—divinyl benzene beads. In the third group, designated as Group III, no filler at all was used, the range of porosities being obtained by using increasingly larger particle sizes to form the specimens. It is seen that the lowest porosity specimens of Groups I and II (in which no filler was used) also comprise the lowest porosity specimens in Group III.

The range of porosities for each group could be divided into subgroups of the same nominal porosity. Because of the large total number of specimens measured, 293, it was more convenient and also facilitated clarity of presentation, to show the data in terms of these subgroups rather than in terms of individual specimens. In some cases, however, when

<sup>1</sup> Figures in brackets indicate the literature references at the end of this paper.

it was believed to be important, statistical analysis was performed on the basis of individual specimens rather than on the basis of subgroups.

The first three columns of table 1 give the specimen designation, number of specimens, and average porosity in each subgroup having the same nominal porosity. The fourth column gives the standard deviation of the porosity of each subgroup. The first two numbers of the specimen designation indicate the particle size and the third number indicates the nominal percentage by volume of filler used. (i.e., 0-2-6 means that the particle size was from 0 to 2  $\mu$  and 6 percent filler was used, 12-24-0 means that particle size was from 12 to 24  $\mu$  and no filler used).

It is also noted from the table that in Group III, the largest particle size (24 to 44 $\mu$ ) resulted in specimens of slightly (but not significantly) lower average porosity (26.08%) than those of the next smaller particle size (13-24 $\mu$ ) which gave specimens having an average porosity of 26.19 percent.

After firing, the specimens were ground to the shape of rectangular bars about  $6 \times \frac{1}{2} \times \frac{3}{4}$  in. The dimensions of each of the finished specimens<sup>2</sup> were uniform to 0.001 in.

Spectrochemical analysis on samples from representative subgroups showed the following impurities: —Al, about 0.01 percent, Si, <0.01 percent, Ni, about 0.005 percent, Mg, <0.005 percent, Fe, <0.001 percent, Sn, present in one sample (7-13-0-7), <0.005 percent. Elements looked for and the presence of which was questionable were Ag and Ca. Elements looked for and not detected were Au, B, Ba, Be, Bi, Co, Cr, Pb, Sb, Ti, V. There appeared to be no significant chemical differences between the different groups and subgroups of specimens. Also

the purity of the starting powder, as measured on one group (0 to 2 $\mu$ ) was not significantly different from that of the finished specimens.

## 2.2. Method

The elastic moduli were determined by the dynamic resonance method previously described [9]. Resonance frequencies were determined to an accuracy of about 1 part in 4,000. For each specimen, the fundamental of four different resonance frequencies was determined. These were

- (1) flexural, flatwise vibration
- (2) flexural, edgewise vibration
- (3) longitudinal
- (4) torsional.

Young's modulus was computed independently from the first three types of vibration ( $Y_1$ ,  $Y_2$ ,  $Y_3$ , respectively) and the shear modulus was computed from the torsional mode. The equations for these computations have also been previously described [9]. The time involved in making these numerous and rather cumbersome calculations ( $293 \times 4 = 1,172$  calculations), as well as most other analysis of the data, was considerably reduced by the use of an automatic computer.

The porosity,  $P$ , in volume fraction of pores, was obtained from the equation,

$$P = 1 - \frac{\rho_s}{\rho_0}$$

where  $\rho_0$ , the theoretical or zero porosity density, is taken as 10.0 g/cm<sup>3</sup>.<sup>3</sup> and  $\rho_s$ , the density of a particular specimen, was obtained from the mass, and volume, calculated from the dimensions.

<sup>2</sup> The starting ThO<sub>2</sub> powder was supplied by the Norton Co., Worcester, Mass.; the particle separation was done by Dr. S. C. Lyons of the Georgia Kaolin Co.; the cold pressing and sintering was done by Norton Co., and the grinding to the final dimensions was done at NBS.

<sup>3</sup> This value is based on the X-ray data of Lang and Knudsen [10], who measured ThO<sub>2</sub> from the same source as used here, obtaining 10.01 g/cm<sup>3</sup> and the A.S.T.M. value (also based on X-rays) of Swanson and Tatge [11] who give 9.991 g/cm<sup>3</sup> on high purity ThO<sub>2</sub>.

TABLE 1. Elastic constants and porosities of thoria specimens of this investigation

	Specimens	Number <i>n</i>	Porosity	$\sigma(P)$ <sup>a</sup>	Young's modulus (flatwise) <i>Y</i> <sub>1</sub>	$\sigma(Y_1)$ <sup>a</sup>	Shear modulus <i>G</i>	$\sigma(G)$ <sup>a</sup>	Poisson's <sup>b</sup> ratio $\mu$	Young's modulus (edgewise) <i>Y</i> <sub>2</sub>	$\sigma(Y_2)$ <sup>a</sup>	Young's modulus (Longitudi- nal) <i>Y</i> <sub>3</sub>	$\sigma(Y_3)$ <sup>a</sup>
			%		Kilobars		Kilobars			Kilobars		Kilobars	
Group I.....	0-2-0	29	3.73	0.09	2296	7	894.1	2.3	0.284	2293	9	2296	7
	0-2-6	6	7.97	.06	1992	18	785.1	5.4	.269	1985	17	2004	19
	0-2-12	5	13.74	.04	1520	94	620.7	26.3	.225	1543	84	1565	84
	0-2-18	6	19.15	.20	1029	83	461.0	20.4	.112	1049	78	1073	78
	0-2-24	3	23.91	.29	779.1	37	365.8	11.0	.065	798.3	39	818.2	35
	0-2-30	2	33.40	.63	167.6	19	114.5	4.3	—, 270	182.1	14	191.7	15
Group II.....	2-4-0	46	7.15	.53	2120	6	830.5	2.0	.276	2117	8	2127	7
	2-4-6	6	12.27	.12	1835	3	724.0	1.3	.267	1835	4	1841	4
	2-4-12	5	16.43	.10	1604	17	638.4	3.1	.256	1609	11	1611	12
	2-4-18	5	22.05	.48	1248	18	507.6	4.5	.229	1261	16	1257	11
	2-4-24	6	28.50	.37	816.6	39	353.3	7.9	.156	829.4	36	827.9	35
	2-4-30	6	33.36	.61	681.0	48	294.8	15.5	.155	692.7	53	691.1	44
	2-4-36	6	39.44	.38	410.6	16	193.4	5.8	.062	428.3	17	429.5	15
Group III.....	4-7-0	39	17.27	.80	1565	8	622.6	2.6	.257	1577	7	1580	7
	7-13-0	39	23.66	.33	1200	6	484.2	2.0	.239	1215	5	1213	20
	13-24-0	40	26.19	.47	1029	9	417.4	3.0	.232	1038	7	1037	7
	24-44-0	44	26.08	.23	985.9	8	401.8	2.7	.227	995.5	6	997.8	6

<sup>a</sup> Indicates standard deviation of value in column immediately to left.

<sup>b</sup> Computed from corresponding  $Y$  and  $G$  values from  $\mu = Y/2G - 1$ .

### 3. Results

The complete data for the specimens are given in table 1. It seems desirable to clarify the following two points at the outset. The first concerns the procedure for obtaining the averages and standard deviations of the porosities and elastic moduli of each subgroup given in table 1. For the porosities, which constitute the independent variable, the standard deviation for a particular subgroup is merely a measure of the range of porosity for that subgroup, and a large value for the standard deviation implies no lack of accuracy in that variable. The average and standard deviation of the porosity of each subgroup, then, was computed directly in the conventional manner. On the other hand, the standard deviation of the associated elastic moduli, the dependent variable, should be a measure of the precision of the data. Consequently, one wishes to know, not the average and standard deviations of the directly determined values of moduli for a subgroup, but rather the average and standard deviation of the moduli that would be associated with the average value of the porosity of that subgroup. This corresponds geometrically to moving the directly determined point for each specimen along a line parallel to the overall porosity-modulus relation for all the specimens of a group until it meets the vertical line through the average porosity for the subgroup in which that specimen is included. This process is represented by the equation,

$$E_a = E_b \pm \Delta P (dE/dP)$$

where  $E$  represents the generalized elastic modulus (whether Young's modulus,  $Y$ , or shear modulus,  $G$ ) and the subscripts,  $a$  and  $b$ , represent the adjusted and unadjusted values of that modulus.  $\Delta P$  is the difference in porosity between the value for a particular specimen (of given  $E_b$ ) and the average for the subgroup containing that specimen. The  $+$  or  $-$  sign in the equation depends upon whether  $E_b$  is at a higher or lower porosity than the average for the subgroup. Average and standard deviations of  $E_a$  were then obtained in the usual manner and are the ones given in table 1.

The values of  $dE/dP$  for the different subgroups used in the equation were obtained in two different ways depending upon whether the subgroups consisted of a small (six or less) or large (about 40) number of specimens.

In the subgroups containing a small number of specimens, where an insufficient number was available to establish a reliable slope for that subgroup, a second degree equation was fitted by least squares to the data representing the particular modulus-temperature relationship for all the individual specimens (not subgroups) comprising a group.  $dE/dP$  for each subgroup was then obtained in the conventional manner, by substituting the average value of porosity for that subgroup into the derivative of the related porosity-modulus equation. The adequacy of these second degree representations of the data will be demonstrated later.

For the larger subgroups, a sufficient number of specimens and a sufficient range of porosity was involved for a satisfactory slope to be computed on the basis of the specimens of each subgroup. A typical plot of such modulus-porosity relation is shown in figure 1. It can be seen from the figure that a linear least squares fit would give a reliable value of  $dE/dP$  for the data. Also, the standard deviation of the ordinate given by the computer along with the least squares equation gives the standard deviation of the elastic modulus directly.

This procedure for both large and small subgroups assumes that  $\Delta P$  is linear over the range of any particular subgroup. This assumption is seen to be justified by figure 1 for a typical large subgroup and would certainly hold for the smaller subgroups having a smaller range of porosities.

The second point concerns the three independently computed values of Young's modulus. It is clear that if the equations for these computations are self-consistent, and the specimens conform to the basic assumptions of the equations, namely that they be homogeneous and macroscopically isotropic, then the values of Young's modulus from the three types of vibration (flatwise flexural, edgewise flexural and longitudinal) must agree within the accuracy of measurement of the relevant parameters (resonance frequency and dimensions). This agreement should be on the order of about 0.2 percent for the specimens of this investigation.

That this is clearly not the case here may be seen from table 2 which gives typical values of Young's modulus computed from these three types of vibration for individual specimens. Since previous work [12, 13] has shown that for materials which are more homogeneous than those used here, annealed glass and steel, the values of Young's modulus computed

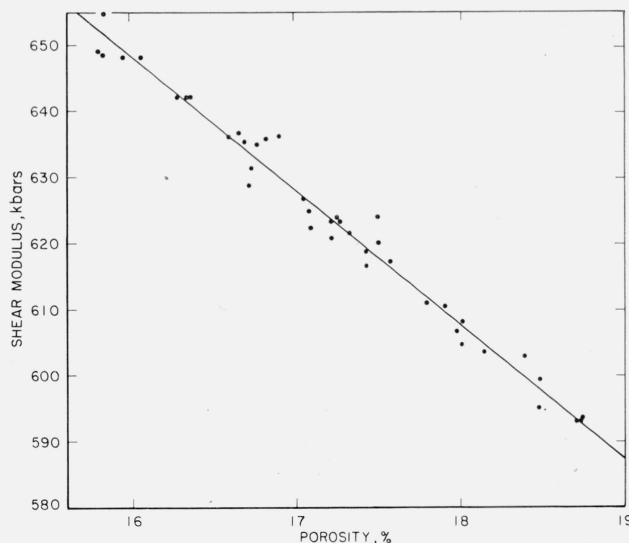


FIGURE 1. Typical data of an elastic modulus versus porosity for a large subgroup 4-7-0.

The line is drawn through the linear least square fit for the data,  
 $G = -2032P + 973$

from these three types of vibration do agree to within the expected figure, one must conclude that it is the lack of uniformity of the specimens (due to nonuniform distribution of the pores throughout the specimens or some other cause) rather than inconsistency in the equations that is responsible for the lack of such agreement found here.

TABLE 2. Typical data showing different values of Young's modulus obtained from three types of vibration

Specimen	Young's modulus		
	$Y_1$	$Y_2$	$Y_3$
	Kilobars	Kilobars	Kilobars
2-4-6-1 <sup>a</sup> ----	1834	1837	1842
2-4-6-2-----	1826	1825	1831
2-4-12-1-----	1634	1634	1640
2-4-12-2-----	1618	1620	1622
2-4-18-1-----	1225	1244	1242
2-4-18-2-----	1241	1248	1248
2-4-24-1-----	795	809	812
2-4-24-2-----	811	831	826
2-4-30-1-----	630	653	654
2-4-30-2-----	632	620	621
2-4-36-1-----	440	458	458
2-4-36-2-----	354	370	374

<sup>a</sup>First three digits indicate starting particle size and nominal porosity. Last digit indicates particular specimen.

This conclusion is strengthened by the following additional information. Almost all the specimens were cut laterally in half and reground for further experimentation after measurement. This work will be described in later publications. A small section was also removed from the middle for microscopic analysis.  $Y_1$  and density for all the cut and reground specimens were obtained in the same manner as already described. Not only did the densities and Young's moduli ( $Y_1$ ) of the two halved specimens not agree with each other but the averages of these values for the two halves often did not agree with those for the specimen from which they were formed. This disagreement was greater for the more porous specimens. In general, the best agreement in  $Y_1$ ,  $Y_2$ , and  $Y_3$  was associated with specimens having the lowest porosities. (This observation is in accordance with the idea that nonuniform distribution of pores is the main cause of lack of uniformity of the specimens, for where the overall porosity is low, any departure from uniformity should have less effect on the bulk specimen.) Lang [3] also found this lack of agreement in  $Y_1$ ,  $Y_2$ , and  $Y_3$ , not only for  $\text{ThO}_2$ , but for sintered materials in general.

Thus, although the precision (the average difference between repeated measurements) of  $Y_1$ ,  $Y_2$ , and  $Y_3$  is usually better than 0.2 percent, nevertheless, the accuracy, using the agreement in these moduli as a criterion, is considerably less than this, being about 1 to 4 percent depending on the porosity; and for the shear modulus,  $G$ , though no such criterion is available, since  $G$  was computed on the basis of only one resonance frequency, the same figure for the accuracy probably applies inasmuch as the same factors are involved. The precision of the values of  $G$  is on the same order as for  $Y_1$ ,  $Y_2$ , and  $Y_3$ .

This lack of agreement in  $Y_1$ ,  $Y_2$ , and  $Y_3$  to within the expected limit and associated lower accuracy for the elastic moduli must not be confused with the standard deviations of the elastic moduli of the subgroups given in table 1. These standard deviations are a measure of the scatter of the points for any given porosity and, although this scatter is undoubtedly a reflection of the nonuniformity of the specimens, it is not a direct measurement of this nonuniformity.

In fact, this scatter, represented by the standard deviations of the elastic moduli in table 1, may mask the real differences in  $Y_1$ ,  $Y_2$ , and  $Y_3$  for individual specimens by making it seem that these values of Young's modulus "agree" if the standard deviations are taken into account. Indeed, it is possible for  $Y_1$ ,  $Y_2$ , and  $Y_3$  to disagree by amounts greater than indicated here and still have standard deviations far less than those in table 1; and conversely, one may have much better agreement in  $Y_1$ ,  $Y_2$ , and  $Y_3$  and yet have standard deviations larger than those in table 1.

This disagreement in  $Y_1$ ,  $Y_2$ , and  $Y_3$  requires that some choice be made as to what value of Young's modulus shall be taken as representative of the specimens in subsequent analysis. One may choose some appropriate average or select that value which is believed most "accurate."  $Y_1$  was finally chosen as the representative value mainly because it is usually the easiest one to obtain experimentally and seems the one most appropriate to compare with shortened specimens which were subsequently fabricated from the large ones, and for which the flatwise flexural resonance frequency is often the only one that can be detected. Further reference to Young's modulus, then, applies to  $Y_1$  and the subscript will be dropped. It is recognized that this choice is somewhat arbitrary but it may be seen from table 1 that had some other value of Young's modulus been selected on some reasonable basis, then, although individual points might vary somewhat, the trends to be shown would not be affected.

The Young's modulus-porosity and shear modulus-porosity relations for all three groups are shown graphically in figures 2 and 3 respectively. Each point for this investigation represents a subgroup given in table 1. It is seen that for both Young's modulus and shear modulus, the data divides itself into two sets. The upper curve in each figure represents the data for Groups II and III while the lower curve is for Group I. The lines drawn through the points are the solutions of the second degree least squares equations for all the individual specimens (not subgroups) of a group. The equation for the upper line in figure 2 is for the specimens of Group II, and is given by

$$Y=3437P^2-6978P+2606.$$

The equation for the lower line in figure 2 is for the specimens of Group I, and is

$$Y=4036P^2-8762P+2621.$$



The shear modulus-porosity equations for Groups II and I, which form the upper and lower curves of figure 3, are respectively,

$$G = 1155P^2 - 2540P + 1008$$

and

$$G = 693.3P^2 - 2885P + 1001.$$

No similar equations for the specimens of Group III were developed because it can be seen from the figures that the equations developed for Group II give a satisfactory fit for Group III as well as the group on which they are based. It is also recalled that the original purpose of these equations was to obtain values of  $dE/dP$  for the small subgroups and all the subgroups of Group III contained a sufficient number of specimens for  $dE/dP$  to be determined on the basis of a linear least squares fit for each subgroup.

On the basis of these equations and the graphs, the "best estimate" of the values of Young's and shear modulus of  $\text{ThO}_2$  at zero porosity,  $Y_0$  and  $G_0$ , (the "theoretical" elastic moduli corresponding to the "theoretical" density) are given as

$$Y_0 = 2610 \text{ kilobars and } G_0 = 1006 \text{ kilobars.}$$

From these values of  $Y_0$  and  $G_0$ , Poisson's ratio at zero porosity,  $\mu_0$  may be computed from the well-known equation for isotropic materials,  $\mu = \frac{Y}{2G} - 1$ , to be 0.297. Values of Poisson's ratio at the different porosities for all subgroups may be similarly computed using the values of  $Y$  and  $G$  for that subgroup. These values are given in table 1 and are plotted in figure 4. The same division in the data previously

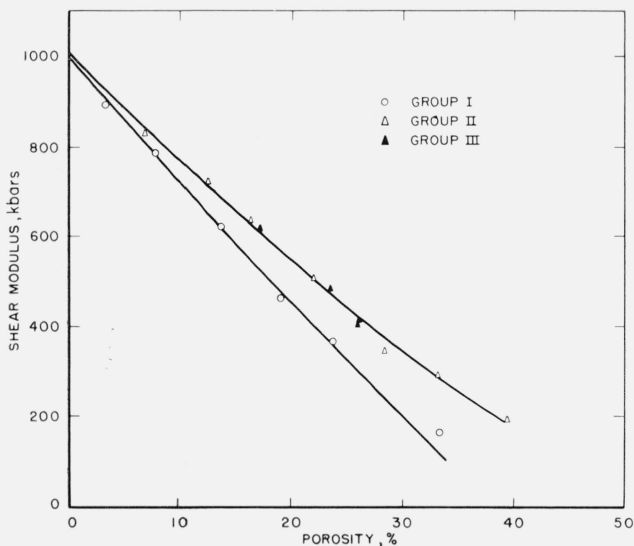


FIGURE 2. *Young's modulus versus porosity for all the  $\text{ThO}_2$  specimens of this investigation.*

Each point represents a subgroup in table 1.

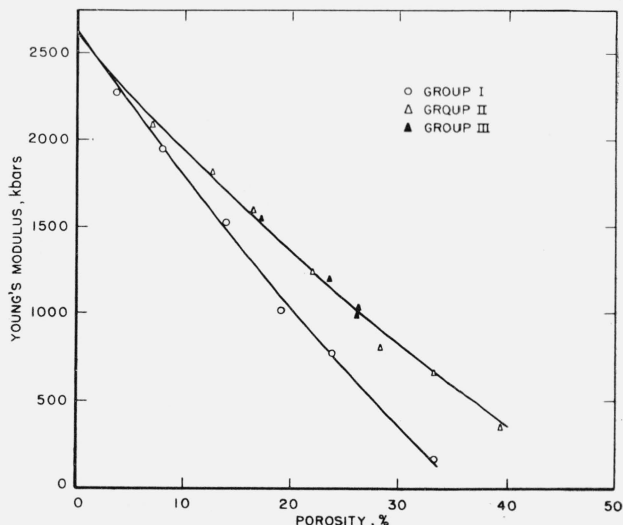


FIGURE 3. *Shear modulus versus porosity for all the  $\text{ThO}_2$  of this investigation.*

Each point represents a subgroup in table 1.

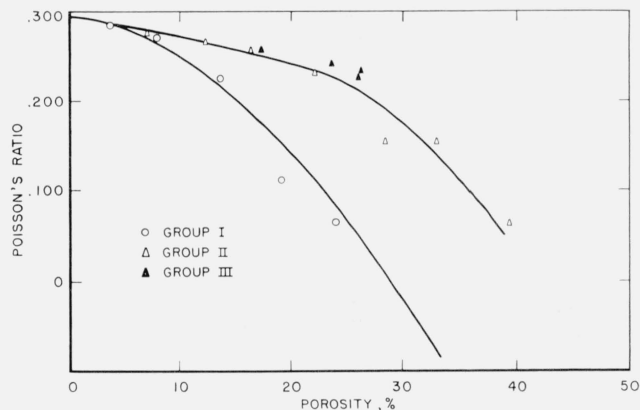


FIGURE 4. *Poisson's ratio versus porosity for all the  $\text{ThO}_2$  specimens of this investigation.*

observed for Young's and the shear modulus as a function of porosity is also seen to hold for Poisson's ratio, the upper curve being for Groups II and III and the lower curve for Group I. Apparently, whatever factor or factors are causing the specimens of Group I to show different Young's and shear modulus-porosity characteristics from those of Groups II and III also manifest themselves for Poisson's ratio as a function of porosity. The greater decrease in Poisson's ratio found for Group I is not a consequence of the fact that the decreases of Young's and the shear modulus for Group I are larger than for Groups II and III, but of the fact that the relative decrease in Young's modulus is greater than the relative decrease in the shear modulus by a larger amount for Group I than for Groups II and III.

The larger scatter in the data for Poisson's ratio than for Young's and the shear modulus is not unexpected, since in the computation of Poisson's ratio from these two moduli, its accuracy is reduced by an order of magnitude from that of Young's and the shear modulus. Thus, the negative value of the 0-2-30 subgroup is probably not correct even though it is in line with the trend for Group I. (In this subgroup,  $\mu$  computed from  $Y_2$  or  $Y_3$ , is also negative but by a smaller amount.)

The tendency for Poisson's ratio to decrease with increasing porosity is in qualitative agreement with Hashin's [8] and Dewey's [4] theoretical predictions. However, the large decrease in the experimental values (above about 15 percent porosity) is not in accordance with theory. As indicated earlier, however, the specimens probably depart from the assumptions of the theories to such an extent that even a qualitative agreement is encouraging.

Using the value of  $Y_0$  for each group, one may plot  $Y_s/Y_0$  where  $Y_s$  is the value of  $Y$  for a specimen at any given porosity, and compare the results of this investigation with those of other investigations on some other sintered materials, plotted on a similar basis. These are shown in figure 5.

Lang's data for  $Al_2O_3$  is typical of a fairly large group for this material, as summarized recently by Knudsen [14]. It is interesting to note that Barducci and Cabarat's [1] results for fritted bronze are in such good agreement with those obtained here for Groups II and III. However, here too, although the decrease in modulus for all these materials is in qualitative agreement with theory, the large differences in  $Y_s/Y_0$  as a function of porosity for the different materials, as well as the two separate curves for different groups of the same material in this investigation, and for  $Al_2O_3$ , indicate that the specimens probably do not conform to the assumptions of the theory and render any attempt at quantitative comparison with the various theoretical formulations (at least, over an extended porosity range) a somewhat dubious procedure.

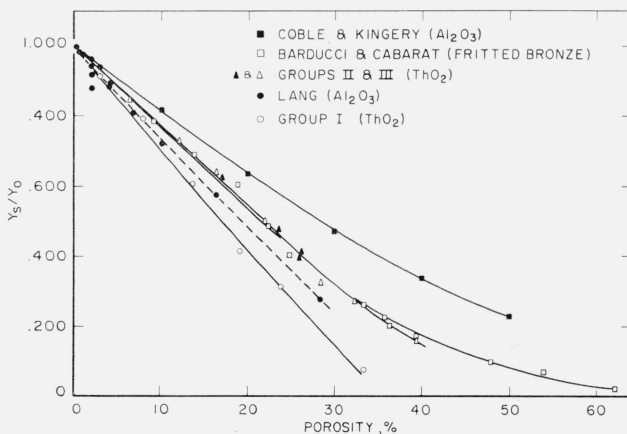


FIGURE 5. Relative change in Young's modulus versus porosity for various experimental investigations with different sintered materials.

Recognizing the limitations involved, it might still be instructive to compare some experimental and theoretical results on the basis of a linear approximation. For this purpose, we consider only the relative slopes at zero porosity,  $-1/E_0 (dE/dP)$ , of the experimental and theoretical relationships. Such a comparison seems realistic since one of the major assumptions of the theories, namely no interaction between pores, is most likely to be realized experimentally as zero porosity is approached. Also, such a comparison should be of more than academic interest because it can be seen from figures 2, 3, and 5 that the porosity-modulus relationships depart only slightly from linearity up to about 15-20 percent porosity which encompasses the range of interest in most practical applications.

These comparisons are shown in tables 3 and 4. A description of the procedures for obtaining the numerical values in these tables is given in the appendix.

TABLE 3. Comparison of some experimental and theoretical values of the relative decrease in the shear modulus,  $-1/G_0 (dG/dP)$ , at zero porosity

Experiment			Theory	
Source	Material		Dewey	Hashin, Mackenzie, Kerner
Group I.....	ThO <sub>2</sub> .....	2.88	1.67	1.90
Groups II and III.....	do.....	2.52	1.67	1.92
Lang.....	Al <sub>2</sub> O <sub>3</sub> .....	2.80	1.67	1.97
Coble and Kingery.....	do.....	2.20	1.67	1.94

TABLE 4. Comparison of some experimental and theoretical values of the relative decrease in Young's modulus with porosity,  $-1/Y_0 (dY/dP)$ , at zero porosity

Experiment			Theory	
Source	Material		Gatto	Hashin, Mackenzie, Kerner
Group I.....	ThO <sub>2</sub> .....	3.34	2.32	2.00
Groups II and III.....	do.....	2.68	2.32	2.01
Cabarot and Barducci.....	Fritted bronze.....	2.68	2.32	-----
Lang.....	Al <sub>2</sub> O <sub>3</sub> .....	3.07	2.32	2.00
Coble and Kingery.....	do.....	2.00	2.32	2.01

Inspection of the tables shows that generally, the relative decrease in elastic moduli found experimentally is greater than the theoretical equations predict. The only exception to this is for the data of Coble and Kingery [2] who obtained a decrease in Young's modulus slightly greater than Gatto's [3] theoretical value. Coble and Kingery [2] also noted that the experimental values of other investigators generally decreased more rapidly with porosity than the theoretical expectations.

Concerning the separation in the porosity-modulus curves for the specimens of Group I from those of Groups II and III, it does not appear that this is due to chemical differences, as has already been noted. Furthermore, the possibility of the effect of different methods of forming the pores, one from

filler and one from different starting particle sizes, must be discounted since the pores of the specimens of Groups II and III were formed in different ways while the pores of Group I were formed in the same way as for Group II.

It has already been suggested [15] that the greater decrease for the experimental values obtained by Lang [3] over the theoretical predictions was due to the fact that the pores were not spherical. Also, the possibility cannot be overlooked that factors other than porosity (such as grain size, grain orientation, nature of grain boundaries, etc.) may also affect the elastic moduli. If however, it is assumed that the more rapid decrease in moduli with increasing porosity for the experimental curves over the theoretical ones is due mainly to the nonsphericity of the pores, then it seems reasonable that the greater decreases in moduli for one set of experimental results over another will be associated with those groups of specimens having pores with greater departures from sphericity. Thus the pores of the specimens of Group I should depart from being spherical to a greater degree than those of Groups II and III. The pores of the specimens of Group I might also be more interconnected in some type of channelized structure than those of Groups II and III. A more definite answer to this problem will probably come from microscopic analysis which will be dealt with in a future publication.

It does seem that since the specimens of Groups II and III were prepared under a wide variety of conditions (more nearly resembling those in actual practice) while the specimens of Group I were prepared under rather specialized conditions, that the elastic constant-porosity curves for Groups II and III are typical for  $\text{ThO}_2$  while the departure of the curves for Group I from this pattern is due to some unusual structural peculiarity in these specimens. Further evidence in support of this conclusion is that the curves for Groups II and III fall more or less in the middle of other experimental relations, and are in better general agreement with various values reported for  $\text{ThO}_2$  [16, 17, 18, 29, 20].

#### 4. Appendix

Experimental values for the relative decrease in Young's and the shear modulus with porosity at zero porosity were obtained in the following manner:

For the specimens of this investigation the values were obtained analytically from the appropriate second degree equations given in the text.

Corresponding values for Lang's results were similarly obtained from second degree equations fitted to his data by Wachtman [15].

The values for Coble and Kingery's results were obtained from a graphical fit to their original data using  $Y_0=3861$  kilobars and  $G_0=1517$  kilobars.

Barducci and Cabarat's value for  $-1/Y_0 (dY/dP)$  was taken as equal to that for Groups II and III because it can be seen from figure 3 that there is no significant difference in these two sets of data at low porosities.

Theoretical values of  $-1/G_0 (dG/dP)$  were obtained in the following manner:

Dewey's expression for the relation between  $G$  and  $P$  is,

$$G/G_0 = 1 - \frac{5}{3}P,$$

then  $-1/G_0 (dG/dP) \cong 1.67$ .

MacKenzie's corresponding equation is

$$G/G_0 = 1 - 5 \left( \frac{3B_0 + 4G_0}{9B_0 + 8G_0} \right) P$$

so that  $-1/G_0 (dG/dP) = 5 \left( \frac{3B_0 + 4G_0}{9B_0 + 8G_0} \right)$ .

Kerner's equation is,

$$G/G_0 = 1 - 5 \left( \frac{3B + 4G}{9B + 8G} \right) P.$$

MacKenzie's and Kerner's equations are seen to differ only in that MacKenzie's equation depends upon  $B$  and  $G$  at zero porosity, whereas Kerner's equation depends upon  $B$  and  $G$  at porosity  $P$ . The two equations become identical as zero porosity is approached so that  $-1/G_0 (dG/dP)$  from either of these equations is the same.

Hashin's equation has been shown by Weil [21] to reduce to the following form as zero porosity is approached,

$$G/G_0 = 1 - \left[ \frac{15(1-\mu)}{7-5\mu} \right] P$$

and  $-1/G_0 (dG/dP) = \left[ \frac{15(1-\mu)}{7-5\mu} \right]$ .

From the well-known equations relating the elastic moduli for isotropic materials, it may also be shown that Hashin's equation is equal to Kerner's and MacKenzie's as zero porosity is approached. Consequently, the numerical values of  $-1/G_0 (dG/dP)$  from Hashin, MacKenzie and Kerner are the same.

Most theoretical formulations (this includes Hashin, MacKenzie, and Kerner) give relations for the bulk modulus as well as the shear modulus as a function of porosity whereas most experimental investigations (such as this one) are in terms of Young's modulus and the shear modulus as a function of porosity. However, from the equations mentioned in the preceding paragraph which are related in such a way that if any two elastic constants are known the others may be computed, one may deduce theoretical equations for Young's modulus as a function of porosity so that experimental and theoretical values of  $-1/Y_0 (dY/dP)$  may be compared.

The equations of MacKenzie, Kerner, and Hashin (Hashin's equation again, as simplified by Weil [21])

for the bulk modulus at very low porosities) are respectively,

$$B/B_0 = 1 - \left(1 + \frac{3B}{4G_0}\right)P,$$

$$B/B_0 = 1 - \left(1 + \frac{3B}{4G}\right)P$$

and

$$B/B_0 = 1 - \frac{3(1-\mu)}{2(1-2\mu)}P.$$

As was the case for the shear modulus relationships, it is obvious that MacKenzie's and Kerner's equations become identical as zero porosity is approached; and it can also be shown that Hashin's equation becomes equivalent to these two as zero porosity is approached.

Following now the procedure just mentioned, one deduces the following equation for Young's modulus from Hashin's equation,

$$Y/Y_0 = (1-P) \left[ 1 - \frac{(1+\mu)}{6(7-5\mu)} (39-45\mu)P + \dots \right]$$

(Higher order terms are negligible for small values of  $P$ .)

Then

$$\begin{aligned} 1/Y_0(dY/dP) = (1-P) & \left[ -\frac{(1+\mu)}{6(7-5\mu)} (39-45\mu) \right] \\ & - \left[ 1 - \frac{(1+\mu)}{6(7-5\mu)} (39-45\mu)P \right] \end{aligned}$$

and at zero porosity

$$-1/Y_0(dY/dP) = \left[ \frac{(1+\mu)}{6(7-5\mu)} (39-45\mu) + 1 \right].$$

Since Kerner's, MacKenzie's, and Hashin's equations for the bulk modulus are equivalent as zero porosity is approached, the numerical values of  $-1/Y_0(dY/dP)$  from the above equation would also apply to the other two.

The values of  $B_0$  and  $\mu_0$  used in these equations were derived from the more directly determined values of  $Y_0$  and  $G_0$ .

Dewey also gives an equation for  $Y$  as a function of  $P$  but this equation is not consistent with her relations for  $G$  and  $\mu$  as a function of  $P$ , and is not used.

Gatto's value of  $-1/Y_0(dY/dP)$  was derived from his graph which is the same as the one used by Coble and Kingery.

## 5. References

- [1] S. Barducci and R. Cabarat, Mesures statiques et dynamiques du module de Young de materiaux frites, *Rev. Met.* **LI** [3] 149-153 (1954).
- [2] R. L. Coble and W. D. Kingery, Effect of porosity on physical properties of sintered alumina, *J. Am. Ceram. Soc.* **39** [11] 377-385 (1956).
- [3] S. M. Lang, Properties of high-temperature ceramics and cermet—elasticity and density at room temperature, NBS Mono. No. 6 (1960), *Ceram. Abstr.*, p. 201i (Aug. 1960).
- [4] Jane M. Dewey, The elastic constants of materials loaded with non-rigid fillers, *J. Appl. Phys.* **18** [6] 578-581 (1947).
- [5] J. K. Mackenzie, "The elastic constants of a solid containing spherical holes, *Proc. Phys. Soc. (London)* **63B** [1] 2-11 (1950).
- [6] E. H. Kerner, The elastic and thermo-elastic properties of composite media, *Proc. Phys. Soc. (London)* **69B** 808-813 (1956b).
- [7] F. Gatto, Influence of small cavities on velocity of sound in metals, *Alluminio* **19** [1] 19-26 (1956).
- [8] Zvi Hashin, The elastic moduli of heterogeneous materials, *J. Appl. Mechanics ASME Paper No. 61-WA-39*, Presented at Ann. Mtg. of ASME (N.Y., Nov. 1961).
- [9] S. Spinner and W. E. Tefft, A method for determining mechanical resonance frequencies and for calculating elastic moduli from these frequencies, *Proc. ASTM* **61** 1221-1238 (Phila., Pa., 1961).
- [10] S. M. Lang and F. P. Knudsen, Some physical properties of high density thorium dioxide, *J. Am. Ceram. Soc.* **39** [12] 415-423 (1956).
- [11] H. E. Swanson and Eleanor Tatge, Standard X-ray diffraction powder patterns, Vol. I, NBS Circ. No. 539 (June, 1953), *Ceram. Abstr.* 1956, p. 173c (Aug.).
- [12] S. Spinner, Elastic moduli of glasses by a dynamic method, *J. Am. Ceram. Soc.* **37** [5] 229-234 (1954).
- [13] S. Spinner, T. W. Reichard, and W. E. Tefft, A comparison of experimental and theoretical relations between Young's modulus and the flexural and longitudinal resonance frequencies of uniform bars, *J. Research NBS* **64A** 147 (1960).
- [14] F. P. Knudsen, Effect of porosity on Young's modulus of alumina, *J. Am. Ceram. Soc.* **45** [2] 94-95 (1962).
- [15] J. B. Wachtman, Jr., Mechanical and electrical relaxation of lattice imperfections in a fluorite structure, Doctorate Thesis submitted at University of Maryland (1961).
- [16] I. E. Campbell (editor), High temperature technology, John Wiley & Sons, Inc., 48 (1956) (Personal communication to R. J. Runck from O. J. Whittemore, Jr.).
- [17] J. B. Wachtman, Jr., W. E. Tefft, D. G. Lam, Jr., and C. S. Apstein, Exponential temperature dependence of Young's modulus for several oxides, *Phys. Rev.* **122** [6] 1754-1759 (Jan. 1961).
- [18] James F. Wygant, Elastic and flow properties of dense, pure oxide refractories, *J. Am. Ceram. Soc.* **12** [34] 374-380 (1951).
- [19] C. E. Curtis and J. R. Johnson, Properties of thorium oxide ceramics, *J. Am. Ceram. Soc.* **2** [40] 63-68 (1957).
- [20] N. A. Weil (editor), Studies of the brittle behavior of behavior of ceramic materials, Armour Research Foundation Contract Report No. 8203-17, 82-90 (Feb. 1962).

The authors are indebted to H. J. Foster and W. E. Tefft for valuable assistance in much of the mathematical development in the appendix.

(Paper 67C1-118)